ELSEVIER

www.elsevier.nl/locate/farmac

Il Farmaco 55 (2000) 700–707

IL FARMACO

Physico-chemical and solid-state characterization of secnidazole

Anailien Boza Rivera [a], Rolando González Hernández [a], Héctor Novoa de Armas [a,b,*], Dulce M. Cuéllar Elizástegi [c], Mariló Valdés Losada [d]

[a] *Center of Pharmaceutical Chemistry, Calle 200 y 21, Atabey, Playa, PO Box 16 042 Havana, Cuba CP 11600*
[b] *Katholieke Universiteit Leuven (KU Leuven), Laboratorium voor Analytische Chemie en Medicinale Fysicochemie, Faculteit Farmaceutische Wetenschappen, E. Van Evenstraat 4, 3000 Leuven, Belgium*
[c] *Center of Research and Development of Drugs, Ave. 26, No. 1605, Nuevo Vedado, Havana, Cuba CP 10600*
[d] *MediCuba, Ave. Máximo Gómez No. 1, esquina a Egido, Havana, Cuba*

Received 8 March 2000; accepted 12 September 2000

Abstract

Secnidazole (hydroxy-2-propyl)-1-methyl-2-nitro-5-imidazole) is an antimicrobic agent. This drug has pharmacological activity against intestinal and hepatic amebiasis, giardiasis and vaginal trichomoniasis. This paper shows the physicochemical parameters of secnidazole determined during a preformulation study. The determination of the apparent partition coefficient and the profile of solubility in dependence of pH demonstrate the basic characteristic of the drug. The dissolution assay was performed to evaluate its behavior in water. For this purpose, a new spectrophotometric method, which was linear from 5 to 15 μg/ml, sensitive, precise, accurate and selective, was validated to assay the bulk drug. The evaluation of higroscopicity revealed that the drug is unstable above 54% of relative humidity. Rheological properties, such as porosity, tapped and bulk densities and percentage of compressibility were calculated. Results show a bad rheological characteristic for this drug. DSC curves do not show any physical interaction between the drug and the excipients in the compatibility studies.

Keywords: Secnidazole; Preformulation; Physico-chemical characterization

1. Introduction

Secnidazole (**I**) (α,2-Dimethyl-5-nitro-1*H*-imidazole-1-ethanol; Fig. 1) is structurally related to the commonly used 5-nitroimidazoles metronidazole and tinidazole. These drugs share a common spectrum of activity against anaerobic microorganisms and they appear particularly effective in the treatment of amebiasis, giardiasis, trichomoniasis and bacterial vaginosis. Secnidazole is rapidly and completely absorbed after oral administration and has a longer terminal elimination half-life (17–29 h) than commonly used drugs in this class [1]. In these cases, the treatment with **I** is shorter and significantly more effective than the treatment using other imidazole drugs and the adverse effects are not very drastic [2].

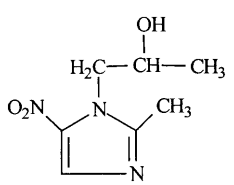

Fig. 1. Chemical structure of secnidazole.

Prior to the preparation of one of the known dosage forms of a drug, it is important to determine certain physicochemical, molecular and other related properties of the bulk drug [3]. These characteristics have not been previously reported for **I**. For this reason, the aim of this paper is to show the results of a study carried out to establish the main properties of **I**, which will be of great utility for the preparation of an appropriate oral solid dosage form.

In the preformulation study it is necessary to have an analytical technique for the quantitative determination of the drug. Previously, a technique was reported to determine 5-nitroimidazole drugs using gas chromatography [4]. Several selective HPLC techniques have been

* Corresponding author.
E-mail address: hector.novoa@farm.kuleuven.ac.be (H. Novoa de Armas).

0014-827X/00/$ - see front matter
PII: S0014-827X(00)00096-3

published for the determination of **I** in finished pharmaceutical preparations and human plasma [5–7]. A spectrophotometric method has been used for the determination of **I** in a pharmaceutical dosage form [8], whereas the spectrophotometric determination of **I** in bulk drugs is described by its reduction to the amino derivative followed by the coupling reaction with 3-methyl-2-benzothiazolinone hydrazone in the presence of ceric ammonium sulfate and measurement of the absorbance at 640 nm [9]. In this work, a new spectrophotometric technique was developed and validated for the quantitative determination of **I** in bulk drugs.

2. Material and methods

2.1. Materials and reagents

Secnidazole bulk drug (purity: 100.27%; water content: $(5.21 \pm 1.26)\%$), supplied by Chemos S.A. (Switzerland), was used to determine physicochemical, molecular and other related properties of the secnidazole bulk drug. Secnidazole supplied by Farchemia S.r.l. (Italy) was used as working reference standard (purity: 101.07%; water content: $(5.40 \pm 0.76)\%$). The quality control of these products is guaranteed and certified by its producers, using control tests for identification (UV and IR spectrophotometry), purity (acid–base titration) and water content (method of K. Fischer).

Monobasic and dibasic potassium phosphate, sodium hydroxide, hydrochloric acid, chloroform of analytical grade and potassium bromide of spectroscopic grade were from Merck (G-Darmstadt, Germany).

2.2. Analytical method

The UV spectrum of **I** in a 10 μg/ml aqueous solution (PC controlled Pharmacia LKB BioChrom 4060 spectrophotometer) was performed from 200 to 400 nm and absorption maximum was obtained at 319 nm (see Fig. 2). The maximum at this wavelength, also found in the UV spectra of **I** recorded in buffered solutions (pH 1.00, 4.00, 6.88, 9.00 and 10.00), did not shift when pH changed.

Five diluted aqueous standard solutions of **I** (5, 7, 10, 13 and 15 μg/ml) in a range from 50 to 150% of a theoretical concentration of 10 μg/ml were prepared twice a day during three days from a matrix solution of 5 mg/ml. The absorbance values of these solutions, prepared twice a day during three days, were measured at 319 nm. The obtained experimental data were used to determine the required analytical parameters such as linearity, sensitivity, precision and accuracy [10], following reported procedures [11]. Selectivity was carried out comparing the data obtained from pure substance and spiked samples with excipients.

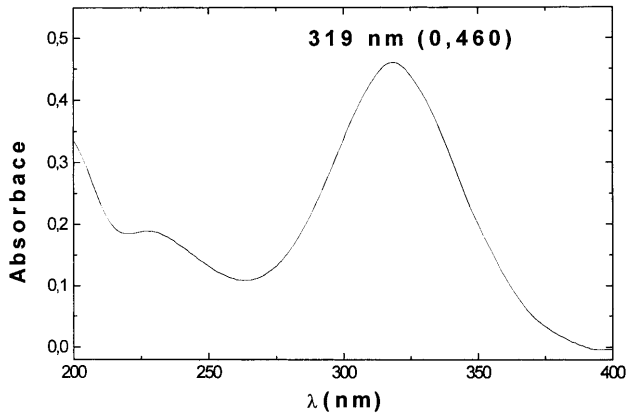

Fig. 2. UV spectrum of secnidazole in aqueous solution of 10 μg/ml.

2.3. Physicochemical characterization

2.3.1. FT-IR spectrophotometry

A sample was prepared and the FT-IR spectrum was recorded on a Bruker IFS 8 FT-IR spectrophotometer by means of a KBr disk containing a few mg of **I**.

2.3.2. X-ray diffraction analysis

Crystals used for X-ray analysis were grown from available bulk drug (see Section 2.1) by slow evaporation from a buffer solution of sodium tetraborate and sodium hydroxide (pH 10.4).

The X-ray powder diffraction pattern was obtained with a Philips P.W. 1710 diffractometer in the 2θ range between 2 and 90° using Ni-filtered Cu Kα radiation; 1.5406 Å (40 kV; 30 mA and 1° min^{-1} scanning rate).

Single crystal data were measured on a Nonius CAD4 automatic four-circle diffractometer using Ni-filtered Cu Kα radiation ($\lambda = 1.5406$ Å). The unit cell dimensions were obtained by a least-squares fit of 50 centered reflections (2θ range: 22–32°).

2.3.3. Solubility measurements

Solubility of **I** bulk drug in aqueous solutions was determined from equilibrated suspensions of saturated solutions (10 ml) at different pH values (1.64, 2.31, 3.42, 4.59, 1.43, 8.5, 9.2, 10.41 and 12.29). The solutions were prepared adding different volumes of HCl 0.1 M or NaOH 0.1 M to a phosphate buffer. All pH values were measured using a calibrated pH meter Methrom 682 (Switzerland).

The samples, prepared in duplicate, were shaken in a mechanical shaker to 50 rpm at 27°C. After a week, they were filtered through 0.45 μm pore size Millipore filters. The filtrates were analyzed spectrophotometrically and the solubility values were determined according to the diluted factors.

2.3.4. Determination of pK_a

The method proposed by Albert and Serjeant [3] was used for the determination of the pK_a. The data from the solubility at different pH values have been used. The intrinsic solubility of **I** (solubility in NaOH 0.1 N aqueous solution) was determined as described above (C_0). The solubility at pH 1.6 has been considered as saturated solubility (C_s). The pK_a value was determined according to the following equation:

$$pK_a = pH + \log \frac{C_s - C_0}{C_0}$$

2.3.5. Apparent partition coefficients

Chloroform (2 ml) was added to 25 ml of aqueous solutions of different pH values (2.31, 4.59, 7.45 and 8.5). These systems were shaken in a magnetic stirrer. After 24 h, they were centrifuged during 15 min at 4000 rpm (HERMLE, Z 320, Germany) and the phases were separated. A 10 mg amount of **I** was added to 5 ml of the aqueous phases and its concentration was determined spectrophotometrically (aqueous phase 1). Aqueous solutions of **I** were then prepared and equal volumes of chloroform were added. These systems were magnetically stirred. After 24 h, they were centrifuged and the final two phases were separated. The concentration of **I** in the aqueous solution was determined spectrophotometrically (aqueous solution 2). The concentration of **I** in the organic phase was determined by the difference between the initial and the final concentration in the aqueous solutions. The apparent partition coefficients were determined from the ratio between the organic and the aqueous concentration of the drug. Chloroform was chosen as partitioning solvent because it is an acidic solvent that partitions most strongly than *n*-octanol, an amphoteric solvent, in the case of weak bases [3].

2.3.6. Dissolution efficiency

A granulometric assay was performed to obtain different particles sizes of **I**. 10 mg from collected fractions of (100–125), (125–250), (250–500) and (500–1000) μm were subjected to a dissolution assay [10] in the apparatus Eureka DT6. Water was selected as a dissolution medium, the temperature was set to (37 ± 0.5)°C by means of a water bath and the mechanical stirring was set to 75 rpm. Fractions of each 3 ml of the vessel content were taken after each 5, 10, 15, 25, 35, 40, 50 and 60 min. This assay was performed twice and dissolved quantities of **I** were determined spectrophotometrically. Dissolution efficiency was determined at 15, 30 and 60 min [12].

2.4. Solid-state physical properties

2.4.1. Morphology and particle size

An optical microscope with an objective of 100 × and an ocular of 10 × (unit of the scale of 1 μm) was used to determine morphological properties and particle size of **I**. For this purpose, a suspension of **I** in liquid petrolatum was prepared. The mean value of diameter by number ($\bar{d}_n$), diameter by weight ($\bar{d}_p$), and diameter of surface volume ($\bar{d}_{vs}$) were determined using Eqs. (1)–(3), respectively:

$$\bar{d}_n = \frac{\sum d_n}{\sum n} \quad (1)$$

$$\bar{d}_p = \frac{\sum nd^4}{nd^3} \quad (2)$$

$$\bar{d}_{vs} = \frac{\sum nd^3}{\sum nd^2} \quad (3)$$

2.4.2. Rheological properties

2.4.2.1. Apparent bulk density. An approximated quantity of **I** was put into a 100 ml graduated cylinder up to 50 ml mark. The cylinder was then weighed to know the mass of the added bulk powder. The apparent bulk density was calculated from the volume occupied by the solid.

2.4.2.2. Apparent tapped density. The bulk drug submitted to a procedure as described in Section 2.4.2.1, was submitted to three series of 500 percussions. The tapped density was determined from the final volume.

2.4.2.3. True density. The powder of **I** was subjected to a high compression pressure (10 ton) during 3 s with a plane die of 13 mm. The obtained tablets were analyzed by means of its mass (m), radii and heights (h) (with a micrometer of 0.05 mm). This assay was replicated five times and the true density (ρ) was calculated using Eq. (4).

$$\rho = \frac{m}{\pi \times r^2 \times h} \quad (4)$$

2.4.2.4. Haussner's index, compressibility and porosity determination. The Haussner's index (H.I.), the percentage of compressibility (%C) and the porosity (e) were determined using Eqs. (5)–(7), respectively

$$\text{H.I.} = \frac{\text{tapped density}}{\text{bulk density}} \quad (5)$$

$$\%C = \frac{\text{tapped density} - \text{bulk density}}{\text{tapped density}} \quad (6)$$

$$e = \left(1 - \frac{\text{bulk density}}{\text{true density}}\right) \quad (7)$$

2.5. Higroscopicity analysis

Three desiccators with 54, 86 and 100% of relative humidity (R.H.) were used to determine the behavior of **I** in presence of water steam. Amounts of 300 mg of dehydrate **I** were weighed and exposed to the desired R.H. The gain in weight of **I** was then determined up to the saturation humidity.

2.6. Compatibility with excipients

Thermal analysis was used to study compatibility of **I** with excipients. Binary mixtures of 1:1 ratio of **I**, Emcompress®, Acdisol®, Aerosil 200 V®, talc, magnesium stearate, and Explotab® were screened by differential scanning calorimetry (Mettler TA 3000 differential scanner calorimeter). Powder samples of approximately 10 mg were weighed in pierced aluminum pans. The heat measurements were performed under static air atmosphere, at a heating rate of 10°C/min and temperature range from 35 and 350°C.

3. Results and discussion

3.1. Spectrophotometric technique

The simple regression analysis was performed using the experimental data obtained in the range of the calibration curve (from 5 to 15 μg/ml). The equation of the fitted model is $y = 0.0089 + 46.72x$. The positive coefficient of correlation obtained (0.9995) shows a relatively strong relationship between the analyte concentration and the absorbance (with a probability higher than 99.9%). The coefficient of determination ($r^2 = 0.999$) shows that the analyte concentration explains the 99.9% of the total variance of absorbance. The coefficient of variation (CV) from the slope of the regression line was lower than the required 2% value [13] and the confidence limits (C.L.) do not include zero. Within C.L. of the intercept, the zero value is included for a 95% of probability. This means that in the concentration range studied, the technique follows the Lambert–Beer law. Since the probability value for lack-of-fit in the ANOVA test is greater than 0.10, the model appears to be adequate for the observed data.

The molar extinction coefficient (ε) corresponding to the slope of the regression curve is 8899.28 l $mol^{-1}cm^{-1}$ (aqueous solution, pH 5.0).

This technique is precise because of the low values obtained for the RSD in the repeatability (within-day repeatability, RSD = 0.4%) and the intermediate precision assay (day to day repeatability, RSD = 2.6% for 5 μg/ml; 1.5% for 10 μg/ml and 1.3% for 15 μg/ml).

The Student's *t*-test, performed to compare the true concentration with those experimentally obtained, shown that the technique is able to determine accurately the concentration of **I**.

No differences were found when the absorption spectra of **I** were compared with those, obtained from spiked samples of **I** within excipients. This explains why the technique is selective to determine **I** in presence of those compounds.

3.2. Physico-chemical characterization

3.2.1. FT-IR spectrum

In the FT-IR spectrum of **I** (Fig. 3), the characteristic peaks corresponding to an OH group (3509.8 cm^{-1}), a NO_2 group (1527.6 and 1358.3 cm^{-1} for the asymmetric and the symmetric bends, respectively), a CH_3 group (1466.4 cm^{-1} for asymmetric bend), a CH_2 group (1489.0 cm^{-1} for scissors bend) and C–N groups (1271.8 cm^{-1}), were identified. This spectrum did not change after dehydration.

3.2.2. X-ray diffraction analysis

X-ray powder diffraction pattern of secnidazole (Fig. 4), show that **I** is a well defined crystalline phase.

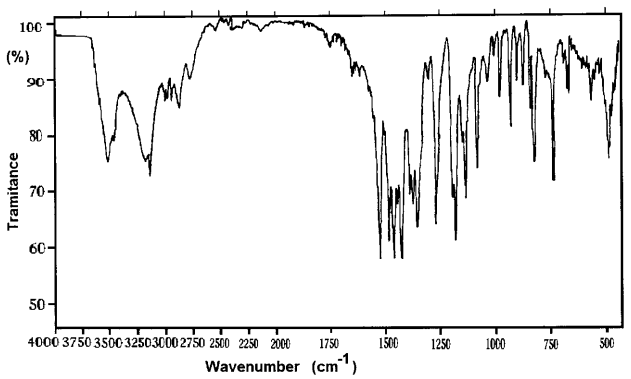

Fig. 3. FT-IR spectrum of secnidazole.

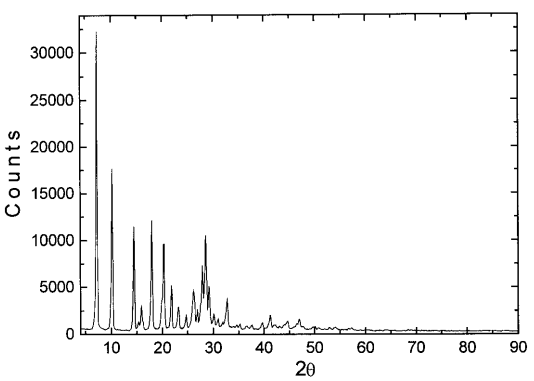

Fig. 4. X-ray powder pattern.

Table 1
Apparent partition coefficient of secnidazole at different pH values

pH	Apparent partition coefficient
2.31	0.22
4.59	0.28
7.45	0.38
8.50	0.40

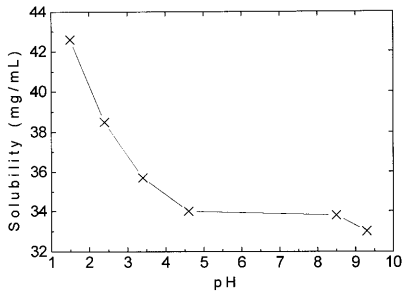

Fig. 5. Solubility diagram of secnidazole in aqueous solutions at different pH values.

Single crystals were obtained by slow evaporation from a buffer solution of sodium tetraborate and sodium hydroxide (pH 10.4), Crystal data for $C_7H_{11}N_3O_3.1/2H_2O$; monoclinic: space group $P2_1/c$ (No. 14); $a = 12.424(2)$, $b = 12.187(2)$ Å, $\beta = 100.09(3)°$, $V = 993.1(3)$ Å^3; $Z = 4$; $D_x = 1.299(2)$, cell weight: 772.75 g, MM: 194.20 g/mol.

The crystallographic study shows the presence of water molecules in the crystal structure. The molecules are held together forming dimers by means of a hydrogen bond between the OH group and a water molecule having a crystallographic occupation site factor of 0.5 [14], this compounds can be assumed as an hemihydrate.

Residues of solvents from the precipitation process can become molecular additions to the crystal and change its habit. The formation of hydrates and solvates have been confused with true polymorphism and led to the term of pseudopolymorphism [3]. Because the experimental powder pattern of the anhydrous form and a calculated pattern from the structure determination (single crystal) of the hemi-hydrate form are similar, we conclude that **I** exhibits pseudopolymorphism [15]. From these results it is deduced that basic aqueous solution should be avoid as recrystallizing solvent to obtain the pseudopolymorph, and the dehydrated product is unstable when is stored in a humid environment.

3.2.3. Solubility

The obtained solutions at different pH values were slightly yellow colored and needle crystals were grown by slow evaporation of solvent. The solubility of **I** clearly increased at low pH values (see Fig. 5). This is due to an increase in the concentration of the ionized species of the drug and a decrease of the unionized form. This behavior is explained by the weak base properties of **I**, which forms a hydrochloride salt in the acid medium.

The high solubility of **I** in aqueous solution can be explained by the presence in the chemical structure of polar groups (OH and NO_2) (see Fig. 1), which are classified as highly and slightly hydrophilic groups, respectively. X-ray crystallography studies also shown that **I** can crystallize having solvent water molecules in the crystal lattice, as described in Section 3.2.2 [14].

The solubility of **I** (~ 33.9 mg/ml at 27°C) is referred to the unionized form and is appropriate to predict a good biodisponibility of the drug.

3.2.4. pK_a calculations

As it was previously mentioned, one method for calculating the pK_a value consists in the application of equation for pH values lower than 11 [3]. Furthermore, the C_s corresponding to these pH values should not exceed 0.1 in order to avoid the effects of the salt's lattice energy. The obtained pK_a value was 1.13 ± 0.09

3.2.5. Apparent partition coefficient

The hydrophilic behavior of **I** and its characteristics of weak base, with predominant unionized form in basic medium, is shown by the slight increase of the apparent partition coefficient with the increasing of the pH (see Table 1). From these results it is also important to note that the additional presence of a positive charge on the molecule (especially at low pH) does not change the hydrophilicity to a large extent. This is probably due to the interaction of ionized form of **I** with chloroform, which is an acidic solvent. However, according to these results an acceptable absorption for this drug can be predicted.

The intrinsic partition coefficient obtained was 0.27. It was calculated from measurements at different pH values by plotting the inverse of apparent partition coefficients against the inverse of the hydrogenionic concentration.

3.2.6. Dissolution efficiency

During the granulometric assay, the formation of agglomerates was observed in the powder. This fact is due to the presence of electrostatic forces between the particles. Nevertheless, it was interesting to perform the dissolution assay with the different fractions to evaluate its dissolution behavior. Table 2 shows a trend from small to large granulometric fractions. For the fraction corresponding to 100–125 μm it is observed an anomalous effect due to the decrease of the dissolution efficiency, when it should be expected an increase. This effect is caused by the high superficial energy among

Table 2
Dissolution efficiency of secnidazole at different times as a function of particle size

Granulometric fractions (μm)	E_d (%)		
	15 min	30 min	60 min
100–125	74.1	75.8	79.0
125–250	94.0	96.0	97.0
250–500	82.0	83.0	85.0
500–1000	68.0	76.0	83.0

particles, which provokes the formation of agglomerates with a relative size larger than the measured originally and therefore diminishes the dissolution efficiency.

This assay demonstrated that **I** has good dissolution properties in water, because almost all the bulk drug was solubilized within 60 min. The best dissolution was obtained with the granulometric fraction of (125–250) μm, resulting in a 97% dissolution of the bulk drug in 60 min, whereas the fraction of (100–125) μm showed the worse dissolution behavior. This is due to the formation of agglomerates, which retards the dissolution.

3.3. Physical properties of the solid state

3.3.1. Morphology and particle size

Fig. 6 is a SEM micrograph of secnidazole. Most particles of **I** have rectangular form rounded at the ends.

Table 3 shows the parameters obtained in the determination of particle size using optical microscopy.

The mean size of the particles of **I** is in the range of (10–30) μm. The distribution of frequencies is close to the normal distribution (see Fig. 7).

The mean value of the geometric diameter of **I**, obtained from the additive distribution (see Fig. 8), was 16.7 μm.

3.3.2. Rheological properties

Table 4 shows the rheological parameters determined for **I**.

The high value of porosity indicates the existence of relatively large empty spaces (72%) among particles. This is due to their rectangular forms (Section 3.3.1). During experiments static currents were noted in the powder. This result explains the low value of the density obtained. As it was expected, a descending order in value was observed for true, tapped and bulk densities [16].

The capacity of **I** to form a compact mass under the action of an external force is moderate (see compressibility value in Table 4).

Because of the value obtained for the Haussner's index (greater than 1.5) [3], it was concluded that the bulk drug has bad flowing properties.

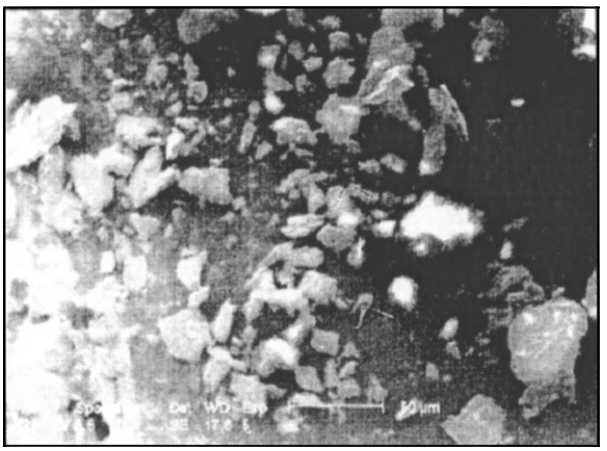

Fig. 6. SEM micrograph of secnidazole.

Table 3
Morphology and particle size of secnidazole determined using optical microscopy

Parameter	Value
Diameter by number (μm)	23.40
Diameter by weight (μm)	44.88
Standard error of weight diameter (%)	1.52
Diameter of surface volume (μm)	38.30

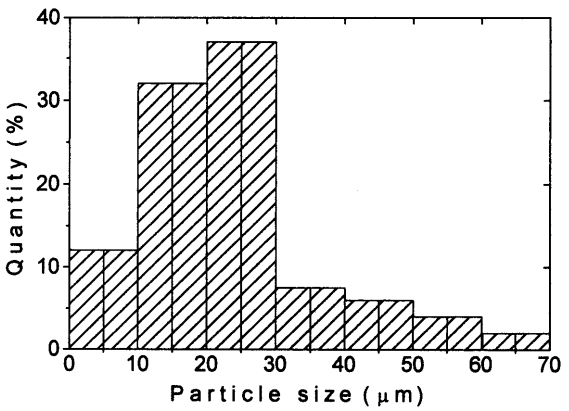

Fig. 7. Histogram of frequencies obtained in the determination of morphology and particle size of secnidazole.

Considering these results, some properties should be improved by adding a gliding agent to the formulation.

3.4. Higroscopicity analysis

It was demonstrated that under conditions of relative humidity (R.H.) of 25 and 54% the bulk drug does not gain weight, whereas at 86% the absorbed water increased (see Fig. 9). Fig. 10 shows the percentage of saturation humidity as a function of the R.H.

These results predict that **I** is physically stable in an atmosphere up to 54% of R.H. at 25°C. This is particularly of interest in countries with tropical climate, where the R.H. is relatively higher than 80% most of the year.

3.5. Compatibility with excipients

Differential scanning calorimetry is particularly valuable in studying the beginning of melting of a compound. The temperature at which the suspected melting endothermic peak begins (first deviation from baseline in the thermogram) is considered to be the beginning of melting. The typical thermogram of **I** is shown in Fig. 11. The calculated melting point was 69.3°C. No additional endotherms were observed from this thermogram, therefore this compound does not give rise to the formation of solvates. This result confirms the one obtained by X-ray experiments shown above.

Basically, the thermal properties of a physical mixture are the sum of the individual components [3]. No change in the melting point, peak shape and area of **I** was observed in the DSC thermograms, obtained from spike samples of **I** in binary 50% mixtures with excipients (69.1°C). For this reason, it was demonstrated that no physico–chemical interactions occurred among **I** and selected excipients.

Table 4
Rheological properties of secnidazole

Parameter	Mean values ± SD
Porosity (%)	72.2 ± 1.68
Bulk density (g/ml)	0.35 ± 0.01
Tapped density (g/ml)	0.53 ± 0.007
True density (g/ml)	1.27 ± 0.01
Compressibility (%)	33.96 ± 0.02
Haussner's index	1.51 ± 0.04
Crystal density (X-ray diffraction) (g/cm^3)	1.299 ± 0.002

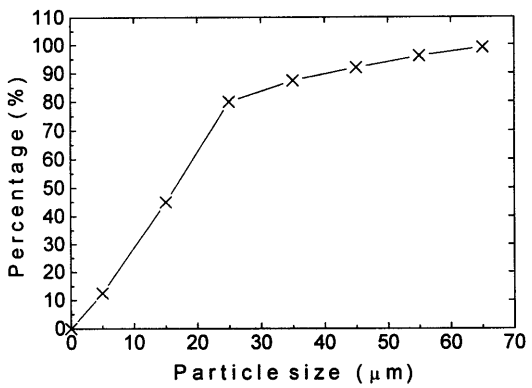

Fig. 8. Additive distribution of the experimental data obtained in the determination of morphology and particle size of secnidazole using optical microscopy.

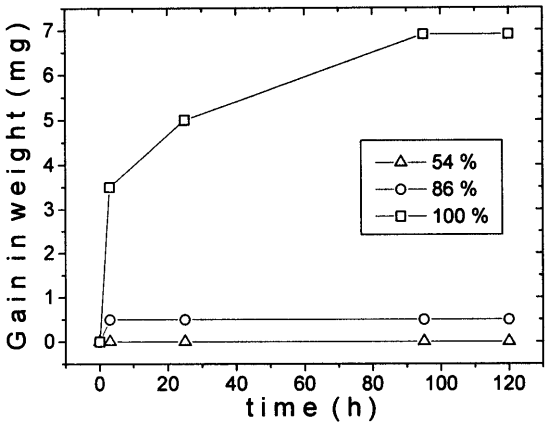

Fig. 9. Plot of gain in weight of secnidazole while it was exposed to different R.H. atmospheres.

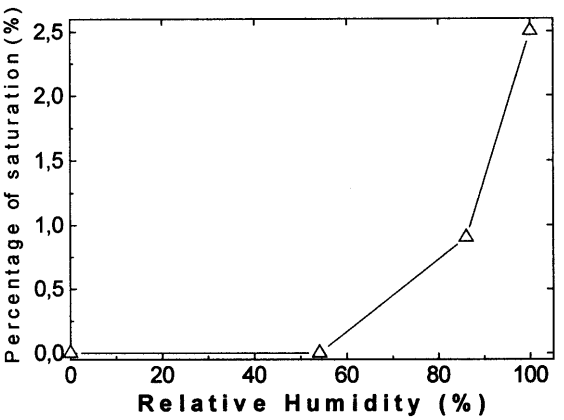

Fig. 10. Plot of percentage of saturation humidity versus relative humidity.

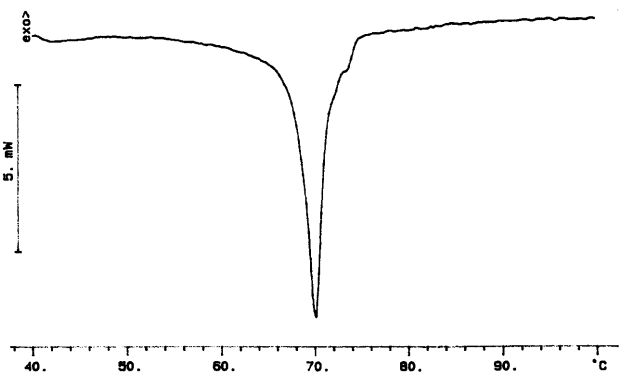

Fig. 11. Typical thermogram of secnidazole bulk drug.

4. Conclusions

The spectrophotometric technique developed is linear, sensitive, precise, accurate and selective for the quantitative determination of the bulk drug, and it is also appropriated for the intended analytical applica-

tions. The solubility values and apparent partition coefficients demonstrated that **I** is a hydrophilic and water soluble drug, which has chemical properties of a weak base. The rheological parameters indicate that this drug does not posses suitable flowing properties and therefore, this should be improved in the formulation process.

The compatibility between the drug and formulation excipients assayed gave satisfactory results.

Acknowledgements

We acknowledge the help from the Center of Research and Development of Drugs (Havana, Cuba) for supporting this work. We highly appreciate Lissette Sordo Martínez for her aid in the experimental work. H. Novoa de Armas wants to thank the K.U. Leuven (Belgium), for its support throughout the IRO Scholarships.

References

[1] J.C. Gillis, L.R. Wiseman, Secnidazole: a review of its antimicrobial activity, pharmacokinetic properties and therapeutic use in the management of protozoal infections and bacterial vaginosis, Drugs 51 (1996) 621–638.
[2] K. Soedin, O. Syukran, A. Fadillah, P. Sidabutar, Comparison between the efficacy of a single dose of secnidazole with a five-day course of tetracycline and clioquinol in the treatment of acute intestinal amebiasis, Pharmaceutica 4 (1985) 251–254.
[3] J.I. Wells, Pharmaceutical preformulation: the physicochemical properties of drug substances, Wiley, New York, 1987.
[4] S.C. Bhatia, V.D. Shanbhag, Electron-capture gas-chromatography assay of 5-nitroimidazole class of antimicrobials in blood, J. Chromatogr. 305 (1984) 325–334.
[5] V.M. Shinde, P.B. Shetkar, Selective determination of enrofloxacin and secnidazole from tablets by reversed phase HPLC, Indian Drugs 33 (1996) 230–231.
[6] S.K. Ravi, M.U.R. Naidu, E.C. Sekhar, T.R.K. Rao, J.C. Shobha, P.U. Rani, K.J. Surya, Rapid and selective analysis of secnidazole in human plasma using high-performance liquid chromatography with ultraviolet detection, J. Chromatogr., Sect. B 691 (1997) 208–211.
[7] R.T. Sane, M. Francis, A.R. Khatri, R. Aamer, Reverse phase high performance liquid chromatographic determination of secnidazole from human plasma, Indian Drugs 35 (1998) 144–146.
[8] B. Jaykar, G. Krishnamoorthy, Spectrophotometric determination of secnidazole in pharmaceutical dosage form, East. Pharm. 39 (1996) 163–164.
[9] M. Narayana, A.V. Hara, D.G. Sankar, N.R. Dutt, Spectrophotometric determination of secnidazole, East. Pharm. 42 (1999) 99–100.
[10] USP 23/NF 18, United States Pharmacopoeial Convention, Rockville, 1995.
[11] B. Castillo, R. González, Protocolo de Validación de métodos analíticos para la cuantificación de fármacos, Rev. Cub. Farm. 30 (1996) 43–51.
[12] M.A. Salvado, J.R. Tico, A. del Pozo, M.J. García, J.M. Sune, Estudio de los procesos de cesión de fármacos. I. Cálculo de parámetros amodelísticos, Cir. Far. 296 (1987) 285–292.
[13] M. Castro, S. Gascón, M. Pujol, J. Ma Sans, L. Vicente, Validation of analytical techniques, Asociación Española de Farmacéuticos de la Industria (AEFI), Sección Catalana, Barcelona, 1989.
[14] H. Novoa, R. González, A. Dago, R. Pomés, N. Li, Estructura cristalina del (hidroxi-2-propil)-1-metil-2-nitro-5-imidazol hemihidratado, Rev. CENIC Ciencias Químicas 28 (1997) 89–92.
[15] H. Novoa, R. González, A. Boza, R. Pomés, I. Herrera, Crystal pseudopolymorphism of secnidazole bulk drug, $C_7H_{11}N_3O_3$, Powder Diffr. 14 (1999) 136–141.
[16] A.I. Torres, Preformulation: Theory and Practice, Universidad Complutense, Madrid, 1995.